Improved Molecular Constants of Acetylene Obtained from the ν_5 Band System

A. Moravec, G. Winnewisser, and K. M. T. Yamada
I. Physikalisches Institut, Universität zu Köln, Köln, West Germany

C. E. Blom
Physikalisch-Chemisches Institut, Justus-Liebig-Universität Gießen, Gießen, West Germany

Z. Naturforsch. **45 a,** 946–952 (1990); received May 12, 1990

A vibration-rotation band system of acetylene of the Π_u bending vibration ν_5 has been recorded with high resolution by a Bruker IFS 120 HR Michelson spectrometer. From the analysis of the hot band of the normal isotopic species, $\nu_4+\nu_5-\nu_4$, and the fundamental band of $HC^{13}CH$ in natural abundance an improved set of constants has been derived. The intensity perturbation due to the *l*-type resonance has been clearly observed in the band system $\nu_4+\nu_5-\nu_4$.

I. Introduction

There exists a number of excellent spectroscopic papers concerning the vibration-rotation spectra of acetylene. Because of its large rotational constant, the spectra of this molecule were fairly well analyzed by Rao and coworkers [1], and Plíva and coworkers [2] using a large grating spectrometer. Recent improvement in the analysis was made by Hietanen and Kauppinen [3], who used their Michelson-type Fourier transform spectrometer.

In the present study we have remeasured the ν_5 band of acetylene using the Gießen Fourier transform spectrometer in order to support our diode laser spectroscopic work near the 700 cm^{-1} wave number region. In this frequency region the acetylene spectrum is rich and thus provides densely spaced calibration points. Several reasons stimulated the analysis of some bands in this spectrum resulting in an improved set of molecular constants: (i) the intrinsically beautiful and textbook like spectra warrant a closer investigation in their own right. As an example we compare in Fig. 1 the FT spectrum of the $HC^{13}CH$ Q-branch near 728 cm^{-1} with the cooled jet diode laser spectrum; (ii) recent supersonic jet spectroscopy shows that several interesting Van-der-Waals complexes can be formed with acetylene [4, 5] and (iii) acetylene is an interstellar molecule which is supposed to play an important role in the interstellar chemistry and can only be observed via its IR spectra [6].

This paper reports the spectrum and analysis of the hot band $\nu_4+\nu_5-\nu_4$ of the main species and of the ν_5 band of $HC^{13}CH$. The high resolution Fourier transform spectrum supplies not only the usual large number of line positions but also gives fairly accurate line intensities of the transitions. In the present study we have used the latter FT property to discuss the intensity perturbation due to the *l*-type resonance.

II. Experimental Procedure and Observed Spectrum

The spectrum was recorded with a Bruker IFS 120 HR vacuum Michelson-type interferometer in Gießen [7]. Using a 17 cm long cell we have measured the spectrum at a pressure of about 85 Pa at room temperature and with a resolution of 0.0036 cm^{-1}. The line positions were calibrated by using CO_2 lines as the wavenumber standard [8]. The recording of the spectrum spans from 410 to 970 cm^{-1}; we covered such a large frequency region in order to use the spectrum to calibrate our diode laser spectrometers. In the present paper we report only on the analysis of a small portion of the observed spectrum. One Q-branch structure is reproduced in Fig. 2 to demonstrate the quality of the spectrum. Industry grade acetylene was used as the sample gas without further purification.

Although the *B* rotational constant of this molecule is very large, about 35 GHz, the observed absorption lines are fairly densely populated due to the excitation

---

Reprint requests to Dr. Koichi M. T. Yamada, I. Physikalisches Institut, Universität zu Köln, D-5000 Köln 41, West Germany.

0932-0784 / 90 / 0800-0946 $ 01.30/0. – Please order a reprint rather than making your own copy.

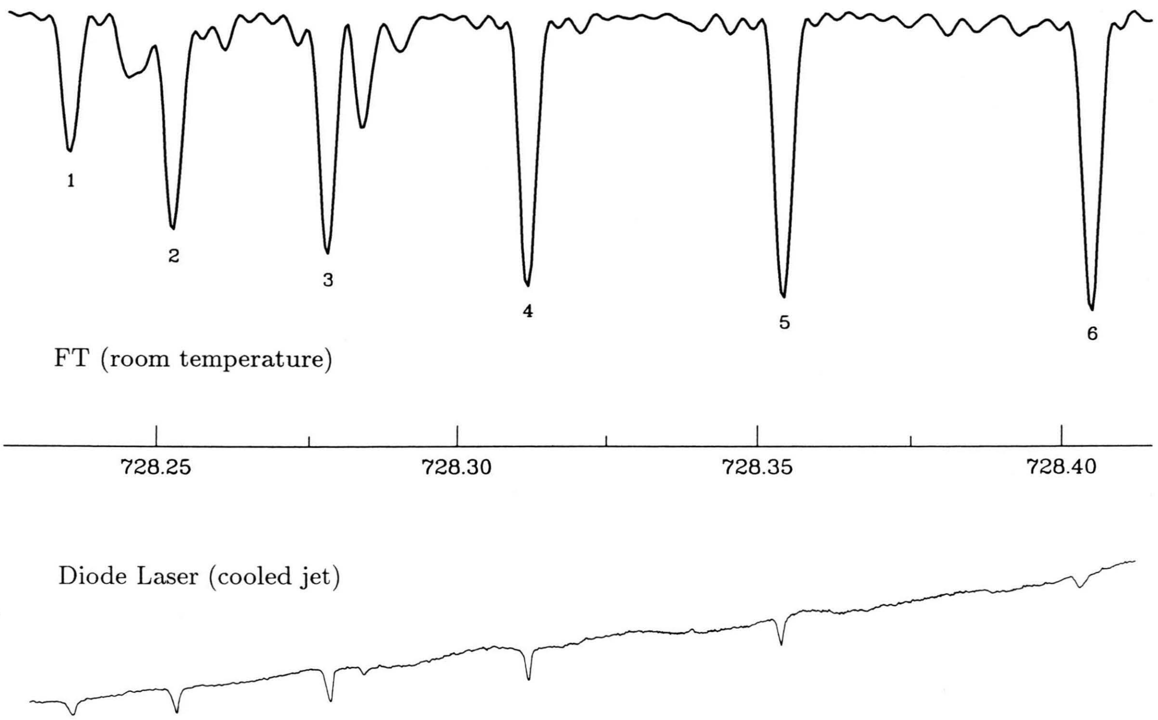

Fig. 1. Comparison of FT and cooled jet diode laser spectrum of the HC^{13}CH $(0, 1^1-(0, 0)$ Q-branch. As expected, no intensity alternation is observed for adjacent *J*-lines.

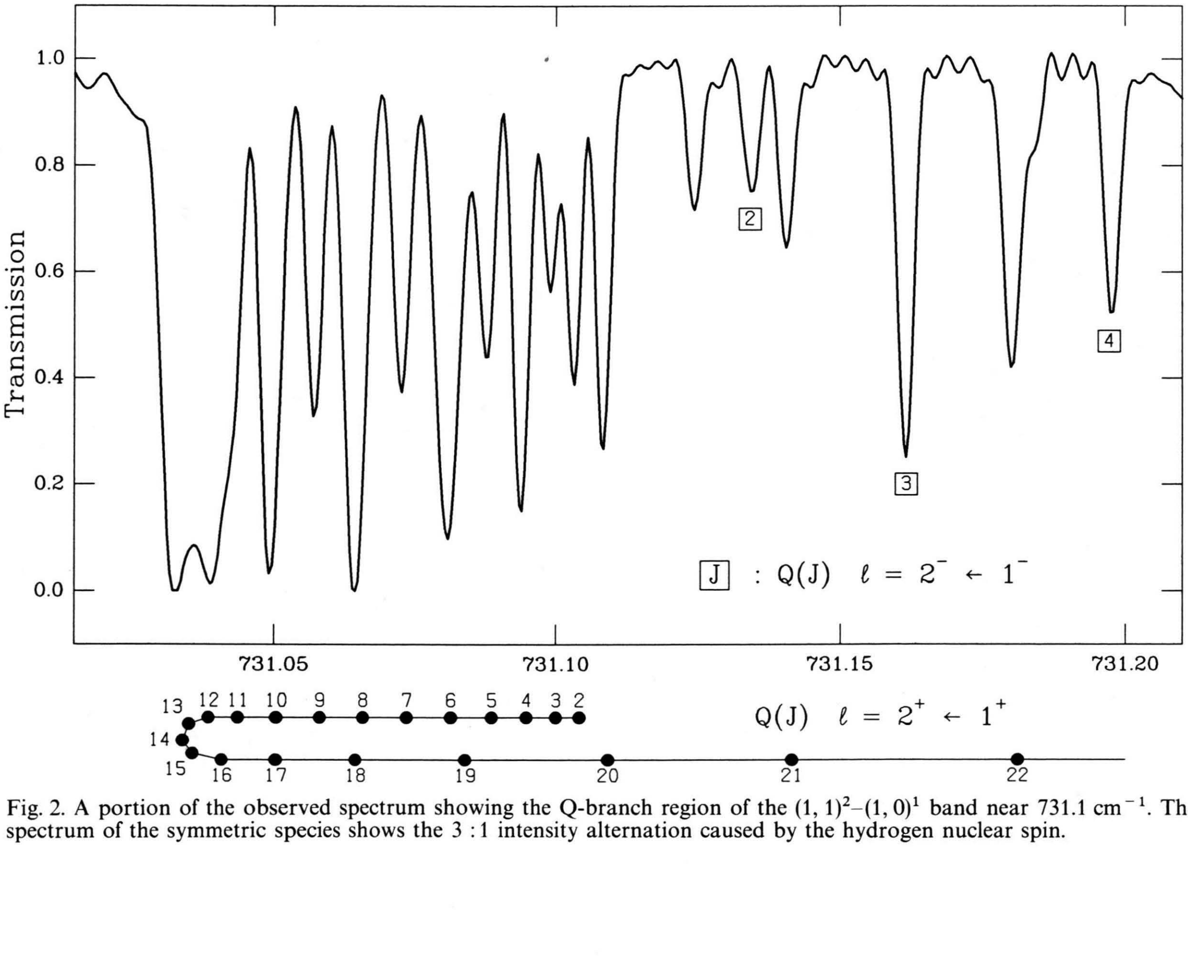

Fig. 2. A portion of the observed spectrum showing the Q-branch region of the $(1, 1)^2-(1, 0)^1$ band near 731.1 cm^{-1}. The spectrum of the symmetric species shows the 3 : 1 intensity alternation caused by the hydrogen nuclear spin.

of many hot and isotope bands. Among them we have analyzed the hot band from the Π_g bending vibration $v_4=1$ state, i.e. the hot band $\nu_4+\nu_5-\nu_4$, because the Π_g bending vibration is infrared inactive and this band is one of the limited sources of information of the $v_4=1$ state. In addition we have analyzed the ν_5 band of HC^{13}CH. We apply the numbering of the normal modes of the symmetric species for this asymmetrical molecule as well, although the center of symmetry is missing as a means to distinguish Π_g and Π_u species.

The assignments of the hot band $\nu_4+\nu_5-\nu_4$ of the normal species and the fundamental ν_5 band of HC^{13}CH were straight forward because the constants available from the literature [3] are good enough to predict the line positions. In addition we could proof the assignments by comparing the FT spectra at room temperature with the diode laser supersonic jet spectra for which the spectra are much simpler because of the low temperature.

III. Analysis

The observed line positions are analyzed by using an effective Hamiltonian of Yamada, Birss, and Aliev [9] for the vibrational states (v_4, v_5)

$$\hat{H} = \hat{h}_\mathrm{d} + \hat{h}_0 + \hat{h}_2 \tag{1}$$

with

$$\begin{aligned}\hat{h}_\mathrm{d} = {} & G_\mathrm{v} + x_{L44}\,\hat{p}^2_{z(4)} + x_{L45}\,\hat{p}_{z(4)}\,\hat{p}_{z(5)} + x_{L55}\,\hat{p}^2_{z(5)} \\ & + \{B_\mathrm{v} + d_{JL}\,\hat{J}_z^2\}(\hat{J}^2-\hat{J}_z^2) - D_\mathrm{v}(\hat{J}^2-\hat{J}_z^2)^2 \\ & + H_\mathrm{v}(\hat{J}^2-\hat{J}_z^2)^3,\end{aligned} \tag{2}$$

$$\begin{aligned}\hat{h}_0 = {} & (r_{45} + r_{J45}\,\hat{J}^2 + r_{JJ45}\,\hat{J}^4) \\ & \cdot(\hat{L}_{++(4)}\,\hat{L}_{--(5)} + \hat{L}_{--(4)}\,\hat{L}_{++(5)}),\end{aligned} \tag{3}$$

$$\begin{aligned}\hat{h}_2 = {} & \tfrac{1}{2}\{\hat{L}_{++(4)}\,\hat{J}_-(q_4 + q_{J4}\,\hat{J}^2 + q_{JJ4}\,\hat{J}^4)\,\hat{J}_- \\ & + \hat{L}_{--(4)}\,\hat{J}_+(q_4 + q_{J4}\,\hat{J}^2 + q_{JJ4}\,\hat{J}^4)\,\hat{J}_+\} \\ & + \tfrac{1}{2}\{\hat{L}_{++(5)}\,\hat{J}_-(q_5 + q_{J5}\,\hat{J}^2 + q_{JJ5}\,\hat{J}^4)\,\hat{J}_- \\ & + \hat{L}_{--(5)}\,\hat{J}_+(q_5 + q_{J5}\,\hat{J}^2 + q_{JJ5}\,\hat{J}^4)\,\hat{J}_+\}.\end{aligned} \tag{4}$$

The operator $\hat{h}_\mathrm{d}$ is diagonal with the vibrational energy G_v, the anharmonicity constants x_{Lij}, the effective rotational constants B_v, the centrifugal distortion constants D_v and H_v, and the l-dependence constant d_{JL}. The operator $\hat{h}_0$ represents the vibrational l-doubling, where r_{45} is the doubling constant, and r_{J45} and r_{JJ45} are its J dependences. The operator $\hat{h}_2$ represents the rotational l-doubling, where q_4 and q_5 are the l-type doubling constants; q_{J4}, q_{J5}, q_{JJ4}, and q_{JJ5} are their J dependences. The notation here is slightly different from those of [9]; we have reversed the order of the suffices for some constants.

In the present paper, the vibrational states are distinguished by the notation (v_4, v_5). When the l-substates have to be distinguished, we use the notation $(v_4, v_5)^{lt}$, where l is the total vibrational angular momentum (l_4+l_5), and t indicates + or − in Wang's combination. The corresponding wavefunctions are given by $|v_4, v_5; l\ t\rangle$. These notations are the same as used for HCCCN and DCCCN by Yamada and coworkers [10, 11]. We repeat here the most important definitions: Wang's linear combinations used in the present study are

$$\begin{aligned}|0,1;1^\pm\rangle &= \{|0^0,1^1;J,1\rangle \pm |0^0,1^{-1};J,-1\rangle\}/\sqrt{2}, \\ |1,0;1^\pm\rangle &= \{|1^1,0^0;J,1\rangle \pm |1^{-1},0^0;J,-1\rangle\}/\sqrt{2}, \\ |1,1;0^\pm\rangle &= \{|1^1,1^{-1};J,0\rangle \pm |1^{-1},1^1;J,0\rangle\}/\sqrt{2}, \\ |1,1;2^\pm\rangle &= \{|1^1,1^1;J,2\rangle \pm |1^{-1},1^{-1};J,-2\rangle\}/\sqrt{2},\end{aligned} \tag{5}$$

where the basis function $|v_4^{l_4}, v_5^{l_5}; J, l\rangle$ is the product of the wavefunctions of the two-dimensional-isotropic oscillators and the symmetric top wavefunction. The phases of the basis wavefunctions are so chosen that

$$\varrho = \delta_4 = \delta_5 = 0 \tag{6}$$

in the sense of Yamada [12].

The (0, 1) − (0, 0) Band of HC^{13}CH

There are well known problems for the sign of the off-diagonal matrix elements of the linear-molecule Hamiltonian. However in the present case the sign of the q_5 constant has been uniquely determined, since we have observed also the well resolved Q-branch transitions in addition to those of the P and R branches. The selection rule for the Q-branch of the (0, 1)−(0, 0) band is f−e, and for the P and R branches e−e. Thus we were able to determine the symmetry and the energy of both of the l-doubling components in the (0, 1) state simultaneously. The analysis of the present data leads to a unique conclusion of positive q_5.

The constants obtained by the least-squares analysis are listed in Table 1. The observed transition wave numbers are listed in Table 2.

Table 1. Spectroscopic parameters of $HC^{13}CH$ obtained in the present study[a].

Constant	Ground state	$v_5 = 1$
G_v/cm^{-1}		729.378362(67)
B_v/MHz	34 429.954(67)	34 489.783(72)
D_v/kHz	46.646(48)	47.289(77)
H_v/Hz		−0.027(33)
q_v/MHz		134.386(13)
q_{Jv}/kHz		−1.090(15)

[a] Numbers in parentheses are uncertainties in one standard deviation in units of the last digit quoted.

The (1, 1) – (1, 0) Band of HCCH

The signs of the off-diagonal constants should be handled carefully in this case. Since the normal species has a center of symmetry, the intensity alternation due to the spin statistics supplies unambiguous information for the symmetry of the energy levels as listed in Table 3. The symmetry combined with the transition frequencies allowed only one choice for the signs of q_4 of the (1, 0) state and r_{45} of the (1, 1) state: positive q_4 and negative r_{45}. From the transition frequencies the signs of the constants q_4 and q_5 of the (1, 1) state are only determinable with the assumption that the constants do not change much for the various vibrational states.

As we can see from the energy matrix of the (1, 1) state in the symmetrized basis, which is by neglecting the higher order off-diagonal terms

$$\begin{array}{c|cccc} & |(1,1)^{0+}\rangle & |(1,1)^{2+}\rangle & |(1,1)^{0-}\rangle & |(1,1)^{2-}\rangle \\ \hline |(1,1)^{0+}\rangle & E_{00}+r_{45} & (q_4+q_5)f & 0 & 0 \\ |(1,1)^{2+}\rangle & & E_{22} & 0 & 0 \\ |(1,1)^{0-}\rangle & & \text{(sym.)} & E_{00}-r_{45} & (q_5-q_4)f \\ |(1,1)^{2-}\rangle & & & & E_{22} \end{array} \tag{6}$$

where E_{ii} are the matrix elements of the diagonal operator $\hat{h}_d$ and

$$f = (1/2)\sqrt{J(J+1)[J(J+1)-2]}\,, \tag{7}$$

we can determine the absolute values of the sum and difference of the two l-type doubling constants from the energy analysis. However, as discussed by Di Lauro and Mills [13] for the Coriolis interaction, we can also determine the signs of the off-diagonal matrix elements from the intensity analysis. The sign information is carried by the eigenfunction and is revealed in the line intensity.

Table 2. Observed line positions of $HC^{13}CH$ in the ν_5 band in cm^{-1}.

J	P		Q		R	
	observed	obs.-calc.	observed	obs.-calc.	observed	obs.-calc.
1			728.23669	30		
2	723.63317	−46	728.25363	28	735.11575	16
3	721.33570	−16	728.27902	24	737.41051	18
4	719.03715	−57	728.31292	23	739.70408	−37
5	716.73915	−8	728.35532	25	741.99825	36
6	714.44084	38	728.40614	22	744.29037	−24
7	712.14096	−46	728.46549	26	746.58226	−34
8	709.84216	2	728.53333	34	748.87394	15
9	707.54270	1	728.60876	−44	751.16373	−43
10	705.24336	27	728.69360	−24	753.45338	−28
11	702.94317	−19	728.78697	6	755.74209	−18
12	700.64398	42			758.02981	−12
13	698.34396	24			760.31663	1
14	696.04392	6	729.11634	−24	762.60260	31
15	693.74388	−16			764.88681	−9
16	691.44465	36			767.17023	−19
17	689.14443	−20	729.52206	41	769.45288	7
18	686.84503	−9	729.67363	27	771.73392	−10
19	684.54542	−36	729.83289	−49	774.01426	25
20	682.24655	−10	730.00172	2	776.29302	26
21	679.94746	−29	730.17815	−15	778.57028	7
22	677.64903	−10	730.36335	20		
23	675.35118	34	730.55635	12	783.12127	20
24	673.05306	19	730.75720	−32	785.39414	−25
25	670.75545	15	730.96684	−16	787.66654	28
26	668.45841	26			789.93679	15
27	666.16104	−39			792.20569	21
28	663.86491	−30	731.64443	15	794.47254	−19
29	661.56986	36			796.73799	−38
30	659.27391	−42	732.13629	7	799.00221	−13
31	656.97980	6	732.39431	7	801.26444	−16
32	654.68601	23	732.66010	−13	803.52537	27
33			732.93420	3		

Table 3. Symmetry and nuclear spin statistics.

			J even	g_I	J odd	g_I
Σ_u^+	$(1,1)^{0+}$	e	+a	3	−s	1
Σ_u^-	$(1,1)^{0-}$	f	−s	1	+a	3
Δ_u^+	$(1,1)^{2+}$	e	+a	3	−s	1
Δ_u^-	$(1,1)^{2-}$	f	−s	1	+a	3
Π_g^-	$(1,0)^{1+}$	f	−a	3	+s	1
Π_g^+	$(1,0)^{1-}$	e	+s	1	−a	3

Figure 3 shows the Boltzmann plot for the observed transitions using the correct perturbed wavefunctions compared with that using unperturbed wavefunctions and that using wavefunctions calculated with improper signs of q_4 and q_5. The Boltzmann plot is a diagram showing the energy dependence of the logarithm of the population obtained from the observed line intensities and the calculated line strength. If the line strengths based on the wavefunctions of the lower and upper states are correct, and if the distribution is boltzmannian, the diagram shows a single straight line, the slope of which is proportional to $(kT)^{-1}$, where T is the thermodynamical temperature of the sample during measurement. Figure 3 (A) shows that the J-dependent intensity anomalies are not taken care of by the normal Hönl-London type intensity expression: the temperature obtained from the 2^+-1^- band is apparently lower than that from the 0^+-1^- band. This effect is caused by the reduction of the intensity of the former band and enhancement of

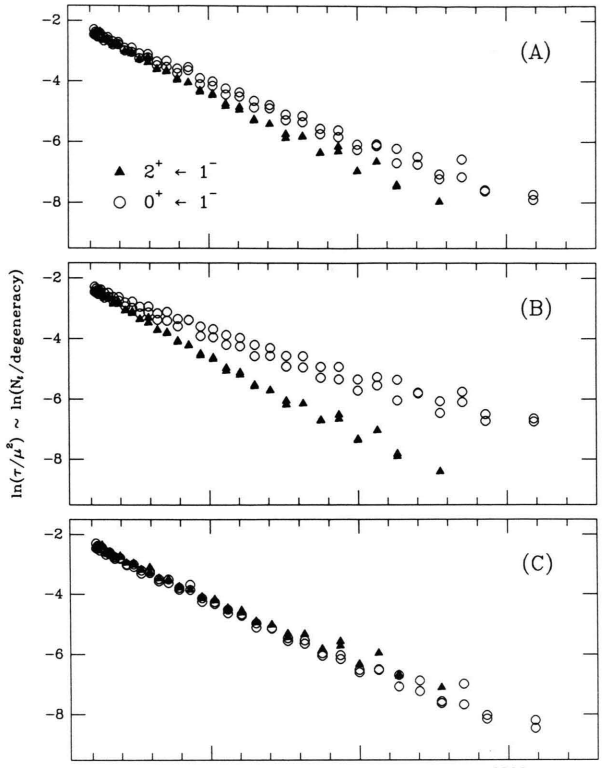

Fig. 3. Boltzmann-plot for P- and R-transitions to (upper) substates $l=0^+$ and $l=2^+$ using (A) the unperturbed wavefunction, (B) an incorrect wavefunction (q_4 and q_5 negative), and (C) the true wavefunction.

Table 4. Spectroscopic parameters of HCCH obtained in the present study [a].

Constant	$(v_4, v_5) = (1, 0)$	$(v_4, v_5) = (1, 1)$
G_v/cm^{-1}	612.871 [b]	1 340.916082(29)
x_{L45}/MHz		198 006.1(10)
B_v/MHz	35 313.548(32)	35 383.795(34)
d_{JL}/MHz		−3.3906(47)
D_v/kHz	49.641(23)	50.372(22)
q_4/MHz	156.827(13)	159.72(11)
q_{J4}/kHz	−1.213(35)	−1.280(66)
q_{JJ4}/Hz	0.026(23)	
q_5/MHz		143.377(55)
q_{J5}/kHz		−1.131(39)
r_{45}/MHz		−187 033.3(13)
r_J/MHz		5.8696(79)
r_{JJ}/kHz		−0.1458(77)

[a] Numbers in parentheses are uncertainties in one standard deviation in units of the last digit quoted.

[b] K. F. Palmer, M. E. Mickelson, and K. N. Rao, J. Mol. Spectrosc. **44**, 131 (1972).

Table 5. Observed line positions of HCCH in the $\nu_4+\nu_5-\nu_4$ band in cm^{-1}: transitions from $l=1^+$ to $l=0$ substate*.

J	P		Q		R	
	observed	obs.- calc.	observed	obs.- calc.	observed	obs.- calc.
1	726.49586	−5			733.57657	24
2	724.13371	−20			735.93429	−18
3	721.77143	39			738.29195	40
4	719.40721	−15			740.64792	41
5	717.04279	−9			743.00225	−7
6	714.67724	−41			745.35587	−6
7	712.31143	−28			747.70793	−36
8	709.94537	27	716.36479	−13	750.05938	2
9	707.57810	26	716.35886	40	752.40935	26
10	705.20958	−39	716.34959	−35	754.75789	46
11	702.84159	6	716.33890	−6	757.10412	−20
12	700.47224	−30	716.32542	37	759.44991	17
13	698.10341	37	716.30794	20	761.79351	−10
14	695.73322	17	716.28681	33	764.13586	−3
15	693.36256	−5	716.26079	9	766.47615	−38
16	690.99133	−41	716.22956	−25	768.81525	−21
17	688.62047	−1	716.19362	41	771.15235	−29
18	686.24907	23	716.15004	−18	773.48840	39
19	683.87712	26	716.10025	5	775.82165	14
20	681.50454	−2	716.04215	−33	778.15311	1
21	679.13222	28	715.97644	7	780.48271	3
22	676.75925	19	715.90099	−22	782.81062	40
23	674.38646	54	715.81636	5	785.13593	28
24	672.01220	−34	715.72145	42	787.45877	−13
25	669.63892	−2	715.61495	20	789.78001	9
26	667.26507	−5	715.49655	−33	792.09887	24
27	664.89060	−53	715.36682	−2	794.41453	−44
28	662.51692	−3	715.22426	13	796.72870	−16
29	660.14269	7			799.04055	32
30	657.76847	35	714.89854	−33	801.34882	−21
32	653.01880	8			805.95874	17
34					810.55679	−7

* In this table and following tables, parity of upper state is determined by the selection rules: e–e and f–f for P- and R-branches and e–f for Q-branches.

Table 6. Observed line positions of HCCH in the $\nu_4+\nu_5-\nu_4$ band in cm^{-1}: transitions from $l=1^-$ to $l=0$ substate.

J	P		Q		R	
	observed	obs.-calc.	observed	obs.-calc.	observed	obs.-calc.
1	714.02846	−39	728.86641	−11	721.11141	−17
2	711.68881	25			723.49320	37
3	709.35862	2	728.91394	−17	725.88367	−35
4	707.03885	−8	728.95215	−2	728.28430	−61
5	704.72957	10			730.69495	−32
6	702.43005	−3	729.05658	−20	733.11448	−31
7	700.14037	−21			735.54308	−7
8	697.86076	0	729.19916	−16	737.98023	29
9	695.59059	24			740.42528	52
10	693.32923	17			732.87698	−14
11	691.07697	44	729.48441	39	745.33667	13
12	688.83235	−2	729.59758	−17	747.80213	−31
13	686.59580	−37	729.72116	30	750.27477	49
14	684.36776	32			752.75161	20
15	682.14589	19	729.99495	−17	755.23320	1
16	679.93022	−17	730.14615	−7	757.71928	33
17	677.72116	20	730.30678	18	760.20777	−22
18	675.51660	−19	730.47618	−5	762.69933	−24
19	673.31769	42	730.65516	9	765.19283	−16
20	671.12145	−32	730.84282	−26	767.68714	−36
21	668.92935	−27			770.18199	−38
22	666.74013	−6			772.67721	33
23	664.55271	−8	731.46148	−33	775.16980	−51
24	662.36674	−6	731.68614	0	777.66216	20
25	660.18175	18	731.91908	−36	780.15140	20
26	657.99672	22	732.16166	−1	782.63708	−30
27	655.81106	5	732.41259	−17	785.11982	−12
28	653.62452	−4	732.67248	−20	787.59811	−24
29	651.43673	9	732.94146	9	790.07239	27
30	649.24629	−52			792.54099	17
31	647.05492	27	733.50491	9	795.00426	19
32	644.86018	34	733.79935	−11	797.46173	17
33	642.66215	11	734.10232	−32	799.91288	−13
34			734.41464	36		
35	638.25651	−14			804.79693	−9

Table 7. Observed line positions of HCCH in the $\nu_4+\nu_5-\nu_4$ band in cm^{-1}: transitions from $l=1^+$ to $l=2$ substate.

J	P		Q		R	
	observed	obs.-calc.	observed	obs.-calc.	observed	obs.-calc.
1					735.82593	−40
2			731.10438	16	738.18307	4
3	724.02073	−31	731.10002	−8	740.53801	−16
4	721.65598	7	731.09502	23	742.89167	−6
5	719.28967	17			745.24321	−47
6	716.92187	0			747.59355	−41
7	714.55332	25	731.07374	6	749.94274	18
8	712.18306	−7			752.28902	−41
9	709.81200	−11	731.05757	−30	754.63420	−34
10	707.44011	7			756.97740	−45
11	705.06732	35			759.31955	21
12	702.69269	−27			761.65891	−7
13	700.31796	−9			763.99641	−31
14	697.94221	−8			766.33295	39
15	695.56541	−31			768.66675	31
16	693.18840	−1			770.99876	40
17	690.81022	−18			773.32806	−21
18	688.43170	−5			775.65654	38
19	686.05281	32			777.98240	40
20	683.67265	−5	731.10960	26	780.30563	−13
21	681.29205	−38	731.14140	−17	782.62714	−28
22	678.91181	8			784.94704	8
23	676.53102	36			787.26435	−1
24	674.14956	29	731.28496	−26	789.57917	−43
25	671.76739	−26	731.35081	−9	791.89241	−25
26	669.38551	−31	731.42615	−32	794.20387	36
27	667.00372	−15			796.51218	2
28	664.62197	13	731.60943	−2	798.81802	−56
29	662.23940	−41			801.12299	24
30	659.85770	−14			803.42466	0
31			731.97022	−14	805.72508	77
32	655.09446	11	732.11549	32	808.02162	−5
34			732.44294	−14	812.60943	−6
36					817.18812	5

the latter by the mixing of the wavefunctions due to the *l*-type resonance. If we correct this effect, we obtain Fig. 3 (C): both bands show a consistent temperature. If we use incorrect sign of the *q*'s, the inconsistence in the temperature increases: this is shown in Figure 3 (B).

By using the Boltzmann plot for all possible choices we have determined uniquely the value (including its sign) of q_4 and q_5 in the (1, 1) vibrational states. The constants thus determined by a least-squares analysis are listed in Table 4. The measured transitions are contained in Tables 5–8.

IV. Conclusion

We report here improved spectroscopic constants of $HC^{13}CH$ in the ground and $v_5=1$ states, and those of HCCH in the $v_4=1$ and $(v_4, v_5)=(1, 1)$ states. The present results are consistent with values quoted in the literature, especially they are in a good agreement with Hietanen and Kauppinen [3]. The present work has been carried out with slightly better resolution and consequently better precision.

The line intensities also supply important information about the molecular constants. In the present study it is shown that one can determine the sign of the *l*-type resonance interaction constants by using the intensity anomaly. In the other words, we have found that the *l*-type resonance interaction produces an unignorable amount of intensity change. Since this resonance is a common interaction for linear molecules, i.e. an inherent interaction and not accidental, we would like to stress that the *l*-type resonance effect has to be always taken into account in the intensity analysis of a linear molecule.

Acknowledgements

Authors wish to express their thanks to Mr. K. Lattner for his excellent assistance in operating the FT spectrometer. The present work was supported in part by the Deutsche Forschungsgemeinschaft both in Köln (through grant SFB 301) and in Gießen.

Table 8. Observed line positions of HCCH in the $\nu_4+\nu_5-\nu_4$ band in cm^{-1}: transitions from $l=1^-$ to $l=2$ substate.

J	P		Q		R	
	observed	obs.-calc.	observed	obs.-calc.	observed	obs.-calc.
1					735.83709	26
2			731.13519	−38	738.21457	−4
3	724.08406	21	731.16273	7	740.60173	18
4	721.76111	39	731.19822	−57	742.99762	−15
5	719.44677	−24	731.24421	26	745.40359	15
6	717.14249	−45	731.29845	32	747.81885	10
7	714.84898	23	731.36142	7	750.24402	5
8	712.56510	39	731.43325	−34	752.67969	33
9	710.29074	−43	731.51496	11	755.12557	31
10	708.02874	26	731.60537	24	757.58227	23
11	705.77726	22	731.70477	33	760.05027	18
12	703.53676	−53	731.81304	28	762.52996	10
13	701.30943	−29	731.93024	15	765.02221	39
14	699.09480	−6			767.52616	−32
15	696.89332	7	732.19203	24	770.04411	−27
16	694.70538	−9	732.33584	−30	772.57647	40
17	692.53205	−10	732.48944	−6	775.12186	−29
18	690.37380	−12	732.65195	9	777.68331	10
19	688.23182	37			780.26020	35
20	686.10540	−1	733.00366	9	782.85296	26
21	683.99674	25	733.19282	−8	785.46192	−44
22	681.90521	−18	733.39163	40	788.08916	−28
23	679.83261	−17	733.59883	28	790.73420	−30
24	677.77956	21	733.81476	−9	793.39830	19
25	675.74618	42	734.03969	−44	796.08112	33
26	673.73213	−51	734.27433	−8	798.78303	0
27	671.74080	20	734.51774	9	801.50530	3
28			734.77012	24	804.24768	−22
29	667.82238	42	735.03157	48	807.01078	−48
30			735.30108	−21		
31			735.58013	−33	812.60166	39
32			735.86879	18		
33			736.16542	−32		

[1] K. F. Palmer, M. E. Mickelson, and K. N. Rao, J. Mol. Spectrosc. **44,** 131 (1972).

[2] J. Plíva, J. Mol. Spectrosc. **44,** 165 (1972).

[3] J. Hietanen and J. Kauppinen, Mol. Phys. **42,** 411 (1981).

[4] M. Takami, Y. Ohshima, S. Yamamoto, and Y. Matsumoto, Faraday Discuss. Chem. Soc. **84,** 1 (1988).

[5] R. L. De Leon and J. S. Muenter, J. Chem. Phys. **72,** 6020 (1980).

[6] G. Winnewisser and E. Herbst, in: Organic Molecules in Space, Topics in Current Chemistry **139,** Springer-Verlag, Berlin 1987, pp. 119–172.

[7] G. M. Plummer, G. Winnewisser, M. Winnewisser, J. Hahn, and K. Reinartz, J. Mol. Spectrosc. **126,** 255 (1987). – M. Birk, M. Winnewisser, and E. A. Cohen, J. Mol. Spectrosc. **136,** 402 (1989).

[8] G. Guelachvili and K. N. Rao, in: Handbook of Infrared Standards, Academic Press, Orlando, Florida, USA 1986.

[9] K. M. T. Yamada, F. W. Birss, and M. R. Aliev, J. Mol. Spectrosc. **112,** 347 (1985).

[10] K. M. T. Yamada and R. A. Creswell, J. Mol. Spectrosc. **116,** 384 (1986).

[11] G. M. Plummer, D. Mauer, K. M. T. Yamada, and K. Möller, J. Mol. Spectrosc. **130,** 407 (1988).

[12] K. Yamada, Z. Naturforsch. **38a,** 821 (1983).

[13] C. Di Lauro and I. M. Mills, J. Mol. Spectrosc. **21,** 386 (1966).